DOI: 10.1002/cbic.200800238

Spin-Label EPR on α-Synuclein Reveals Differences in the Membrane Binding Affinity of the Two Antiparallel Helices

Malte Drescher,[a, b] Frans Godschalk,[a] Gertjan Veldhuis,[c] Bart D. van Rooijen,[c] Vinod Subramaniam,*[c] and Martina Huber*[a]

The putative function of the Parkinson's disease-related protein α-Synuclein (αS) is thought to involve membrane binding. Therefore, the interaction of αS with membranes composed of zwitterionic (POPC) and anionic (POPG) lipids was investigated through the mobility of spin labels attached to the protein. Differently labelled variants of αS were produced, containing a spin label at positions 9, 18 (both helix 1), 69, 90 (both helix 2), and 140 (C terminus). Protein binding to POPC/POPG vesicles for all but αS140 resulted in two mobility components with correlation times of 0.5 and 3 ns, for POPG mole fractions >0.4. Monitoring these components as a function of the POPG mole fraction revealed that at low negative-charge densities helix 1 is more tightly bound than helix 2; this indicates a partially bound form of αS. Thus, the interaction of αS with membranes of low charge densities might be initiated at helix 1. The local binding information thus obtained gives a more differentiated picture of the affinity of αS to membranes. These findings contribute to our understanding of the details and structural consequences of αS–membrane interactions.

Introduction

The major component of Lewy bodies—a key feature of Parkinson's disease—is α-synuclein (αS), a small soluble protein of 140 amino acids (Figure 1).[1–4] Its central role in the disease brought αS into the focus of scientific research several years ago, but many aspects, including its physiological function, are not yet understood. Monomeric αS in solution is largely unfolded, with a slight tendency to form secondary structure.[5–7] The biological functions of αS are hypothesised to be closely related to membrane binding.[1,8,9] Thus, information on details of the membrane association of αS, including the structure of the membrane-bound protein is the subject of intense research.

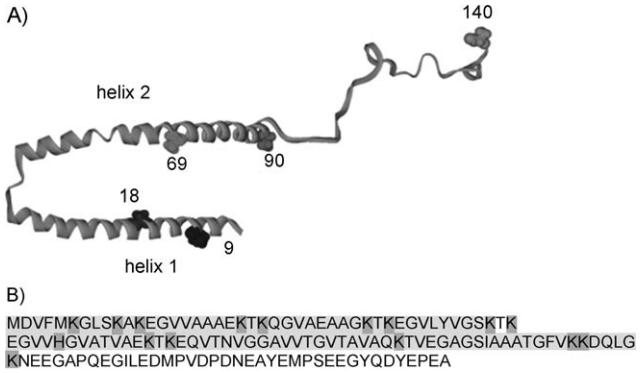

Figure 1. A) Schematic representation of the two helices of α-synuclein (αS) and the position of residues mutated. Structural model from micelle-bound αS.[25] B) Amino acid sequence of wild-type αS. Putative helical segments 1 and 2 are marked in grey.

Different techniques have been employed to elucidate the binding of αS to lipids. Binding of αS to anionic vesicles was detected by gel filtration chromatography.[10] Preferential binding of αS to anionic vesicles and α-helical structure of the bound αS was detected by CD spectroscopy.[11,12] Fluorescence correlation spectroscopy (FCS) was used to measure real-time binding of αS to large unilamellar vesicles (LUVs), again revealing preferential binding to negatively charged lipids.[13] Also, the effect of different lipids and of the protein/lipid ratio was investigated. The binding was found to be cooperative, to have an electrostatic component, and a model was proposed to explain the effect of the protein/lipid ratio.[13]

Whereas binding to LUVs and even multilamellar vesicles (MLVs) was reported, higher binding affinities to small unilamellar vesicles (SUVs) suggested a preference for membranes with a smaller radius of curvature.[10,13–15] The interaction of αS with spin-labelled lipids revealed different membrane affinities of αS mutants linked to early onset familial Parkinson's disease.[16,17]

[a] *Dr. M. Drescher, F. Godschalk, Dr. M. Huber*
Department of Molecular Physics, Leiden University
P.O. Box 9504, 2300 RA Leiden (The Netherlands)
Fax: (+31) 71-527-5819
E-mail: mhuber@molphys.leidenuniv.nl

[b] *Dr. M. Drescher*
Present address: Department of Chemistry, University of Konstanz
Universitätsstrasse 10, Box 706, 78457 Konstanz (Germany)

[c] *Dr. G. Veldhuis, B. D. van Rooijen, Prof. Dr. V. Subramaniam*
Biophysical Engineering, MESA+ Institute for Nanotechnology and
Institute for Biomedical Technology, University of Twente
P.O. Box 217, 7500 AE Enschede (The Netherlands)
Fax: (+31) 53-4891105
E-mail: v.subramaniam@tnw.utwente.nl

Structural information on vesicle-bound αS derived from solution NMR experiments revealed that the N-terminal part of αS (approximately residues 1–100) is able to associate with the lipid–water interface and to adopt an α-helical structure, while the C terminus remains unstructured and unbound.[5,18] Qualitatively, the conformation of the N-terminal part of the molecule bound to micelles has been characterised as two distinct, antiparallel amphipathic α-helices connected by a short linker region consisting of residues 42–44. The helices exhibit an unusual 11/3 periodicity and are denoted as helices 1 and 2.[18–22] The large size and associated slow tumbling rates of the complex of αS bound to even small lipid vesicles make a direct NMR structure determination difficult, limiting the amount of structural information on vesicle-bound αS. Several approaches employing spin-label EPR have been published.[23–26] In one case spin-labelled αS was investigated in the presence of SUVs. Line broadening was observed and attributed to immobilisation of the spin label by membrane interaction.[23] The broad part of the spectrum was investigated, revealing that the spin-label properties agree with the 11/3 α-helix model.

In this work we have used the site-specific mutagenesis spin-labelling approach pioneered by Hubbell et al.[27] and 9 GHz, continuous wave (cw) EPR to determine the mobility of the spin labels at different positions of αS within helices 1 and 2 as a function of membrane composition. By using single-cysteine mutants, spin labels have been introduced at positions 9, 18, 69, 90 and 140, and their interactions with SUVs composed of different ratios of zwitterionic (POPC) and negatively charged (POPG) lipids have been studied.

We find that the membrane affinities of the two helices of αS differ. In particular, at low charge densities, binding occurs preferentially around helix 1, that is, the helix closer to the N-terminal part of αS.

Results

Spin-labelled αS in solution gives rise to EPR spectra with narrow lines, thus indicating a high mobility (rotation correlation time $\tau_r < 1$ ns) of the spin label (Figure 2A and B; all spectra are shown as first derivative). In the presence of negatively charged SUVs, the spectra of almost all mutants show drastic changes (Figure 2C). The spectra consist of more than one component, one of which is clearly broadened relative to the main component in spectra of αS in solution (see features at 334.5 and 335.3 mT, Figure 2C). Broadening is indicative of a lower mobility of the spin label. Only the spectra of αS140 remained unchanged upon addition of SUVs (Figure 2A). This is expected as residue 140 is the final residue of αS, located at the C terminus of αS, a region that was shown not to interact with the lipid membrane.[5,28]

All spectra were analysed quantitatively by spectral-lineshape simulations. The spectra of αS in the absence of liposomes are well described by a superposition of two components S_1 and S_2, where S_1 corresponds to the spectrum of the free spin label ([(1-oxyl-2,2,5,5-tetramethylpyrroline-3-methyl)-methanethiosulfonate]—MTSL) measured independently. In the presence of SUVs, an additional component S_3 is needed,

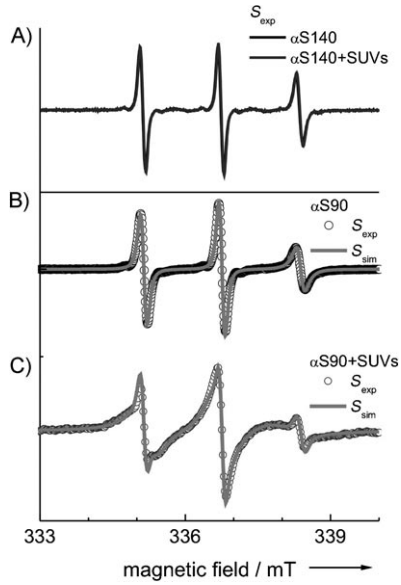

Figure 2. A) EPR spectra of αS140 in the absence or presence of negatively charged SUVs. EPR spectra of αS90 and simulations in the B) absence and C) presence of negatively charged SUVs. The simulations (——) are composed of the components S_1 and S_2 (B) and additionally S_3 (C); see text for details.

corresponding to the broadened part of the spectra. The shape of component S_3 and the prefactors *a*, *b*, and *c* are determined by least square fits to the data according to $S_{sim} = aS_1 + bS_2 + cS_3$.

This approach is visualised in Figure 3. Owing to normalisation of S_i, the values of *a*, *b*, *c* (where $a+b+c=1$) express directly the fractions of spins contributing in each case. The width of the spectra can also be expressed as the second moment $\langle \Delta B^2 \rangle$. For S_2, a value of $\langle \Delta B^2 \rangle \approx 2\,\mathrm{mT}^2$ was found, whereas for S_3 $\langle \Delta B^2 \rangle \approx 3\,\mathrm{mT}^2$ (for an interpretation, see the Discussion).

The spectral parameters of the components S_1 and S_2 are listed in Table 1. The parameters of the slow motion contribution S_3 and the parameters *a*–*c* can be found in Table 2. Note

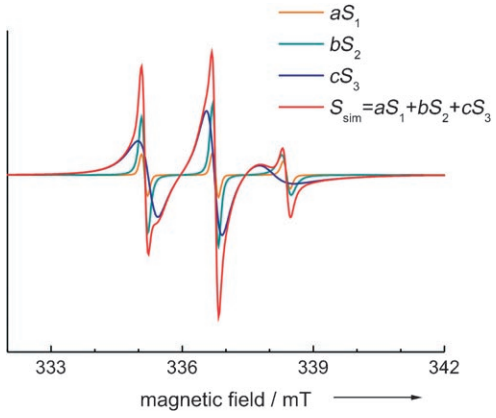

Figure 3. Composition of EPR spectra of αS90 in the presence of SUVs. The weighted sum $S_{sim} = aS_1 + bS_2 + cS_3$ of all three contributions shown corresponds to the simulated spectrum of Figure 2C.

Table 1. Simulation parameters of spectral contribution S_1 and S_2: hyperfine interaction, A_{zz}, and rotational correlation time, τ_r.

	A_{zz} [MHz]	τ_r [ns]
unbound MTSL (S_1)	111 ± 0.5	0.13 ± 0.01
αS9 (S_2)	109.8 ± 0.2	0.59 ± 0.02
αS18 (S_2)	109.6 ± 0.5	0.55 ± 0.02
αS69 (S_2)	109.7 ± 0.2	0.39 ± 0.02
αS90 (S_2)	110.6 ± 0.5	0.41 ± 0.01
αS140 (S_2)	110.4 ± 0.2	0.15 ± 0.01

Table 2. Relevant parameters of spectral contribution S_3. The fractions *a*, *b*, and *c* are given for SUVs containing 100% negatively charged lipids ($\rho = 1$).

	A_{zz} [MHz]	τ_r [ns]	*a*	*b*	*c*
αS9 (S_3)	97 ± 2	3.2 ± 0.2	0.05	0.12	0.83 ± 0.02
αS18 (S_3)	99 ± 2	3.2 ± 0.3	0.03	0.01	0.96 ± 0.01
αS69 (S_3)	106 ± 2	2.9 ± 0.3	0.00	0.01	0.99 ± 0.005
αS90 (S_3)	105 ± 2	2.3 ± 0.2	0.04	0.01	0.95 ± 0.01

that the parameters of the spectra of αS140 are not given in Table 2 as it does not contain component S_3, that is, $c = 0$.

The prefactors *a*, *b*, and *c* of αS in the presence of POPG SUVs (Table 2) show a variation in *c* dependent on the mutant and a small contribution of *b*. The value of *a* is small in all cases (< 5%), indicating that there is only a small amount of free MTSL. Nevertheless, this fraction has narrow lines with large amplitudes and therefore has to be taken into account in the simulation. To study the influence of the charge density of the liposome surface (ρ), the (molar) fraction:

$$\rho = \frac{[\mathrm{POPG}]}{[\mathrm{POPG}] + [\mathrm{POPC}]} \quad (1)$$

of anionic POPG lipids added to zwitterionic POPC was varied. For each mutant, the spectra in the range of $0 \le \rho \le 1$ were measured and simulated by using the unchanged spectral contributions, S_i (Tables 1 and 2) varying only *a*, *b*, and *c*. Figure 4 shows the dependence of fraction *c* on the charge density ρ. Errors were determined as described in the Experimental Section. Repeated measurements of individually prepared samples did not lead to deviations exceeding the displayed error bars.

For $\rho < 0.4$, no slow motion contribution was detected, corresponding to $c = 0$. Simulations showed that fractions of *c* below 30% cannot be detected given the signal-to-noise ratio of the experimental spectra. The relatively low sensitivity of the method to small fractions of *c* comes from the large linewidth of that component. For higher ρ values, the fraction *c* depends on the position of the MTSL label (Table 2) and on the value of ρ. For $\rho > 0.4$ for two of the mutants (αS9 and αS18) the *c* values do not depend on ρ within experimental errors, whereas αS69 and αS90 show a decrease in *c* by up to 15% for decreasing ρ.

In order to obtain further evidence on the interpretation of the spectral components, two experiments were performed.

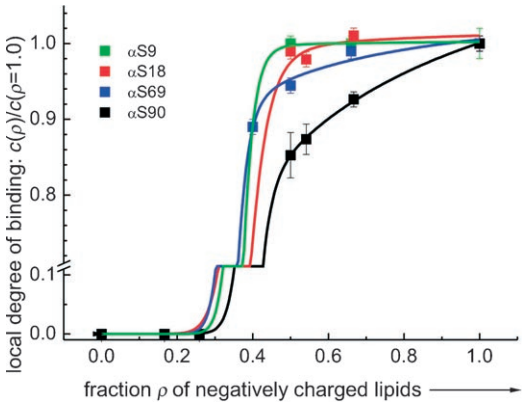

Figure 4. The surface charge density (ρ) of the SUVs can be controlled by varying the content of negatively charged lipids. Fraction *c* of the spectral contribution S_3 is shown for different mutants of αS. Fractions *c* smaller than 0.3 cannot be detected (see text). Fraction *c* reflects directly the local binding degree (see Discussion). For clarity the data points were connected using sigmoid-like curves.

First we tested whether the spectrum of doubly labelled αS was similar to the superposition of the spectra of the respective singly labelled αS. Figure 5A, open circles, shows the experimental spectrum at $\rho = 0.5$ of the double mutant, where both residue 18 and residue 90 (αS18/90) are spin labelled.

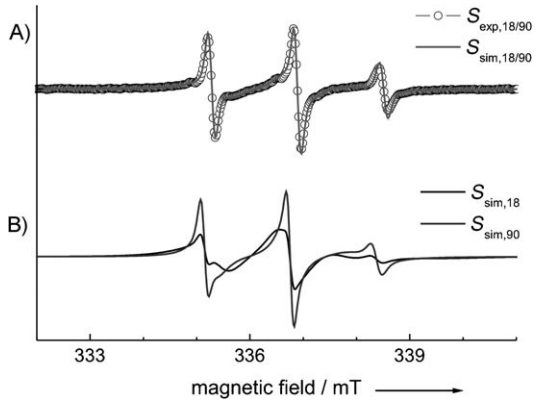

Figure 5. A) The experimental spectrum of the doubly labelled mutant αS18/90 (○) can be described by simulations (——) generated by the sum of the simulations of the corresponding singly labelled mutants αS18 and αS90 including a small adjustment for fraction *a*. B) Spectra of the singly labelled mutants αS18 (——) and αS90 (····).

Adding the spectra of the single mutants αS18 and αS90 (Figure 5B) results in the spectrum shown as a solid line in Figure 5A. It is almost identical to the spectrum of the double mutant. The similarity of the two spectra shows that the values of the prefactors *b* and *c* are an intrinsic property of the spin label at the respective position and not a result of different membrane binding affinities of the mutants.

In the second experiment, a solution of αS90 with POPG/POPC SUVs ($\rho = 0.67$) was subjected to a filtering procedure (Experimental Section) to separate vesicle-bound from unbound αS. The EPR-spectrum of the retentate of the filtration

was identical to that before filtration, and the concentrated filtrate did not reveal any EPR signal. That the mobile fraction *b* in the retentate did not decrease shows that *b* does not stem from αS that is free in solution, but rather that under the specific conditions of the filtration experiment (αS90, $\rho = 0.67$) all of the *b* fraction is due to αS that is bound to the SUVs. At lower ρ values, presumably, S_2 contains contributions from both bound and dissociated αS, a point that is discussed in detail below.

Both experiments show that the fractions *b* and *c* cannot be interpreted as originating from purely free αS in solution and completely membrane bound αS, respectively, and that the membrane affinity of αS is not altered by the spin labelling (see Discussion).

Discussion

The EPR spectra of all mutants of αS are distinct and, with the exception of αS140, reveal clear changes upon interaction with the membrane.

In order to interpret the spectra, line shape simulations using multiple components were performed (see Results). The strategy of simulation for the three components of the spectra of αS with SUVs was as follows. Spectra of αS in the presence of SUVs are composed of the spectra S_1, S_2, and S_3 where S_1 is due to free MTSL and S_2 is the spectrum of the αS mutant in the absence of SUVs (see Results). Fitting the shape of the component S_3 and the ratios *a*, *b*, and *c*, resulted in good agreement with the experimental spectra (see Figure 2). Thus, the fractions *a*, *b*, and *c* and the correlation time τ_r of the slow motion component S_3 can be determined with sufficient accuracy, although subtle differences in hyperfine splitting or correlation time of S_2 in these three-component spectra cannot be detected.

Spin-labelled αS in the absence of vesicles and the component S_2 (fraction *b*) in the presence thereof are characterised by τ_r values (Table 1) close to those of the spin label in unfolded proteins.[29–31] The spectra are similar to those observed earlier and interpreted as monomeric, largely unfolded αS.[24] In the presence of negatively charged SUVs, the spectra of all mutants except αS140 revealed a considerable fraction *c*.

The rotation-correlation time of the component S_3 (fraction *c*) is $\tau_r \approx 2$–3 ns, which is similar to the parameters of spin labels at exposed sites in folded proteins.[23,31] The mobility derived from the second moment $<\Delta B^2>$ is close to that of tertiary interaction sites and helix surface sites.[32] The measured magnitude of τ_r for fraction *c* is much smaller than the τ_r of a lipid vesicle ($\tau_r > 0.5$ μs, calculated from Stokes–Einstein equation) showing that the rotation of the vesicle is much too slow to account for the τ_r observed. Therefore, τ_r reflects residual mobility of the spin label. As fraction *c* is composed of spin labels with reduced mobility, and as that fraction is only observed when SUVs are present, the restricted mobility of the spin labels must stem from the interaction of αS with the SUV, as demonstrated earlier in a study where the broadened component itself was analysed to determine the helix periodicity of the membrane-bound fraction in SUVs containing 30% negatively charged (POPS) and 70% zwitterionic (POPC) lipids.[23]

Before we can interpret the results of αS in the presence of SUVs with spin labels at different amino acid positions, we will take a closer look at the origin of fraction *b* in these experiments. Either, the entire fraction *b* comes from αS that is free in solution, or—as we show is the case—it also contains a contribution of αS that is physically bound to the membrane, but dissociated in the region where the mobility is monitored (Figure 6B and C). Such a fraction can have a mobile spectrum, if the region of αS close to and including the position of the spin label is sufficiently loosened to allow the spin label to rotate so fast that its spectrum cannot be distinguished from that of the spin label of the free αS in solution. The filtration experiment shows that this must be the case for the entire fraction *b* at $\rho = 0.67$ (that is, under the conditions of the filtration experiment), as that fraction does not contain any unbound αS (see Results). Also, the αS140 spectra do not change, independent of whether αS is in contact with a membrane or not, revealing that the mobility at the end of the C terminus of αS is sufficient to give rise to mobile EPR spectra that are indistinguishable from those of αS140 in solution.

In summary, fraction *c* is composed of αS bound to the membrane in such a way that the spin label becomes immobilised. Fraction *b* contains a contribution of αS bound to the membrane such that the spin label is conformationally mobile and (possibly) a contribution of free αS in solution. Different values of *c* observed for the different mutants could, in principle, be an indication that the mutants have different membrane affinities. However, the experiment on the doubly la-

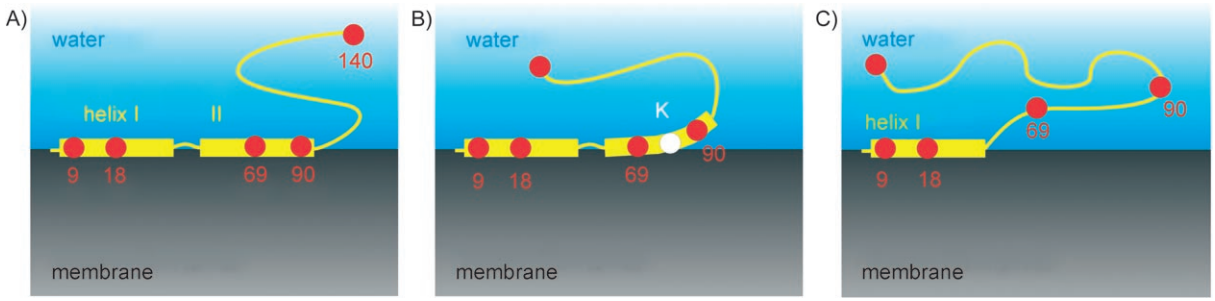

Figure 6. Schematic representation of αS at the membrane–water interface. Positions of spin labels used in this study are depicted as red circles. The following situations can be distinguished: A) Both helices of αS are completely bound to the vesicle. B) Detaching of helix 2 starts from the acidic tail. The cationic residue K80 still bound to the negatively charged membrane is also shown. C) Helix 2 is completely dissociated whereas αS remains bound via helix 1.

belled mutant αS18/90 show that this is not the case (see Results).

Classical binding studies in the literature determine the amount of αS that is completely bound versus the amount that is fully dissociated from the membrane.[13] Fraction *c*, as determined by EPR, is constituted exclusively of membrane-bound αS but fraction *b* also contains bound αS, the amount of which depends on ρ. Therefore, our fraction *c* represents the lower limit for membrane-bound αS. In apparent contrast to that, in binding studies of αS with POPS/POPC lipid mixtures the amount of bound αS is smaller than fraction *c* under similar conditions, but there is good agreement with αS binding to POPA/POPC membranes.[13] Presumably, this is due to the fact that the headgroup of POPG is chemically closer to POPA than to POPS and therefore has a similar affinity for αS than POPG. Below $\rho = 0.26$, in the present study no immobilised fraction is observed, that is, *c* is 0.3 or less (see results). Binding of αS to neutral vesicles was observed,[13] but the amount of αS bound to such vesicles[13] is below the detection limit of our method. In summary, the data presented herein are in good agreement with those obtained from binding studies reported in the literature.

Whereas the interpretation of the fraction *c* discussed in the preceding paragraph enables us to compare the results with traditional binding studies, the true merit of the present method is that *b* and *c* give local information about the binding of the individual sections of αS, that is, binding of the specific region of αS that is close to the spin-labelled residue.

In Figure 4, the variation of the immobilised fraction *c* for four of the mutants is shown as a function of the liposome charge density ρ. Starting at high charge densities, for all positions, the amount of fraction *c* decreases with decreasing values of ρ.

From $\rho = 1.0$ to $\rho = 0.4$, the behaviour is strongly dependent on the position of the spin label; this indicates that certain regions of αS dissociate from the membrane more readily than others. Thus, regions around residues 9 and 18 remain bound at lower membrane charge density than the regions around residues 69 and 90. In that range of ρ, positions 69 and 90 show a clear dependence on ρ, whereas *c* for positions 9 and 18 remain almost the same. We attribute differences in the dependence of *c* on ρ as an effect of nonuniform binding of αS to the membrane surface. Specifically, we suggest that, as the negative charge density decreases, helix 2 dissociates whereas helix 1 remains bound (Figure 6C).

An explanation for the apparent difference in binding of helix 1 and helix 2 could be the distribution of cationic residues (such as lysines) in the sequence of αS. Helix 2 contains fewer cationic residues than helix 1 (Figure 1B) and therefore will have weaker electrostatic interactions with the negatively charged membrane. Therefore, at a lower negative charge density the interaction may be too weak for binding. Even the fact that residue 90 detaches before residue 69 could thus be explained as K80 is a cationic residue right between residues 69 and 90 (Figure 6B). Additionally, the negatively charged tail containing anionic residues is expected to affect the binding of helix 2 nearby.

Conclusions

The EPR approach presented here gives a more differentiated view of the interaction of αS with the membrane than the overall binding constants determined previously by other methods.[10, 13, 33, 34] It suggests that, at lower charge density, the binding affinity of helix 1 is stronger than that of helix 2. This implies that the binding of αS to membranes could be initiated in the N-terminal part of αS and that subtle alterations in the membrane composition could provide a means to manipulate further binding events along the polypeptide.

Experimental Section

Protein expression and labelling: Wild-type αS does not contain any cysteine residues. αS cysteine-mutations at position 9, 18, 69, 90, or 140 as well as a double mutation (18/90) have been introduced using standard biochemical methods. To perform site-directed spin labelling, αS mutants were expressed in *Escherichia coli* strain BL21(DE3) using the pT7–7 expression plasmid (courtesy of the Lansbury Laboratory, Harvard Medical School, Cambridge, MA). Purification procedure of the αS mutants was performed as will be described elsewhere. Prior to labelling, αS mutant proteins were reduced with a 6× molar excess of −SH groups (with DTT) for 30 min at room temperature. Subsequently, samples were desalted with Pierce Zeba 5 mL desalting columns. Immediately, a 6× molar excess of MTSL spin label [(1-oxyl-2,2,5,5-tetramethylpyrroline-3-methyl))-methanethiosulfonate] was added (from a 100 mM stock in MeOH) and incubated for 1 h in the dark at room temperature. After this, free label was removed by using two additional desalting steps. Protein samples were applied onto Microcon YM-100 spin columns to remove any precipitated and/or oligomerised proteins and diluted in buffer (10 mM Tris-HCl, pH 7.4). Spin label concentrations for single-cysteine mutants were 100 μM and for double-cysteine mutants 200 μM. Owing to the high reactivity of the label and the fact that the cysteine residues are freely accessible in the poorly folded structure, near quantitative labelling can be achieved under these conditions.[23] Samples were stored at −80 °C.

Preparation of vesicles: Anionic POPG [1-palmitoyl-2-oleoyl-*sn*-glycero-3-(phosphor-*rac*-(1-glycerol))] and zwitterionic POPC [1-palmitoyl-2-oleoyl-*sn*-glycero-3-phosphocholine] lipids were purchased dissolved in chloroform (Avanti Polar Lipids) and were used without further purification. After mixing chloroform solutions to obtain the desired lipid ratio, the solvent was evaporated by using a gentle stream of dry nitrogen gas. The resulting lipid film was dried under vacuum overnight. After adding Tris-HCl (10 mM), pH 7.4, and incubation of 15 min at room temperature, SUVs (diameter ca. 25 nm) were generated by a minimum of 30 min sonication of larger vesicles.[10]

Preparation of samples: The αS solution was added to the SUV solution; this resulted in a protein/lipid ratio of 1:250 and a final concentration of 100 μM (200 μM) for singly (doubly) labelled mutants, and incubated for at least 0.5 h before being measured. To separate unbound αS from αS bound to SUV, one sample has been filtered using a YM-100.000 membrane (Millipore) in a fixed angle (35°) rotor at 5000 *g* for 60 min. Whereas the concentrate (60 μL) is expected to contain the SUVs and αS that is bound to the SUVs, unbound αS should be found in the filtrate. To check for unbound αS in the filtrate, the filtrate was first concentrated using a 5 kDa filter (Millipore) at 7000 *g* for 60 min and subsequently

measured for EPR signals. EPR spectra of unbound MTSL as well as those of labelled protein in buffer solution not containing liposomes were measured independently.

EPR measurements and analysis: All experiments were performed at room temperature. A Bruker Elexsys E680 X-band spectrometer equipped with a standard rectangular microwave-cavity ER 4102 ST operating in TE_{102}-mode was used.[30] Performing modulated field sweeps containing 1024 data points (sweep time 42 s) a modulation frequency of 100 kHz was used. Modulation amplitude as well as time constant (low pass filter) have been chosen such that the signal was not distorted. Typical values are 0.27 G and 40 ms, respectively. Spectrometer control and data post-processing were performed by the Bruker Xepr software. To simulate the spectra, we used Matlab R2007b (The MathWorks Inc., Natick, MA, USA) and the toolbox EasySpin 2.6.[35] Varying simulation parameters, least-square-fits to experimental data have been performed. For all simulations described in this work $A_{xx}=A_{yy}=13$ MHz and $g=[g_x\ g_y\ g_z]=[2.00906\ 2.00687\ 2.003]$ were chosen.[36] Error margins were determined by manually changing the parameters and to test in which range acceptable simulations of the data were obtained. In order to exclude any saturation effect[13] the protein/lipid ratio was chosen as 1:250 after verifying that changing the ratio of proteins to lipids in the range from 1:250 to 1:100 did not result in any spectral change.

Acknowledgements

We thank Sergey Milikisyants for stimulating discussions. Yvonne Kraan is kindly acknowledged for help in expression and purification of the mutant proteins. This project was supported by Deutsche Forschungsgemeinschaft (DFG) (DR 743/1-1; M.D.) and the Stichting Internationaal Parkinson Fonds (Hoofddorp, The Netherlands; G.V.). This work is part of the research programme of the "Stichting voor Fundamenteel Onderzoek der Materie (FOM)", which is financially supported by the "Nederlandse Organisatie voor Wetenschappelijk Onderzoek (NWO)".

Keywords: EPR spectroscopy · membrane binding · site-directed spin labeling · synuclein

[1] K. Beyer, *Cell Biochem. Biophys.* **2007**, *47*, 285–299.
[2] M. G. Spillantini, M. L. Schmidt, V. M. Y. Lee, J. Q. Trojanowski, R. Jakes, M. Goedert, *Nature* **1997**, *388*, 839–840.
[3] M. Goedert, *Nat. Rev. Neurosci.* **2001**, *2*, 492–501.
[4] M. Goedert, *Clin. Chem. Lab. Med.* **2001**, *39*, 308–312.
[5] D. Eliezer, E. Kutluay, R. Bussell, G. Browne, *J. Mol. Biol.* **2001**, *307*, 1061–1073.
[6] L. C. Serpell, J. Berriman, R. Jakes, M. Goedert, R. A. Crowther, *Proc. Natl. Acad. Sci. USA* **2000**, *97*, 4897–4902.
[7] O. Weinreb, S. Mandel, T. Amit, M. B. H. Youdim, *J. Nutr. Biochem.* **2004**, *15*, 506–516.
[8] J. M. George, H. Jin, W. S. Woods, D. F. Clayton, *Neuron* **1995**, *15*, 361–372.
[9] D. E. Cabin, K. Shimazu, D. Murphy, N. B. Cole, W. Gottschalk, K. L. McIlwain, B. Orrison, A. Chen, C. E. Ellis, R. Paylor, B. Lu, R. L. Nussbaum, *J. Neurosci.* **2002**, *22*, 8797–8807.
[10] W. S. Davidson, A. Jonas, D. F. Clayton, J. M. George, *J. Biol. Chem.* **1998**, *273*, 9443–9449.
[11] W. S. Davidson, A. Jonas, D. F. Clayton, J. M. George, *J. Biol. Chem.* **1998**, *273*, 9443–9449.
[12] E. Jo, J. McLaurin, C. M. Yip, P. George-Hyslop, P. E. Fraser, *J. Biol. Chem.* **2000**, *275*, 34328–34334.
[13] E. Rhoades, T. F. Ramlall, W. W. Webb, D. Eliezer, *Biophys. J.* **2006**, *90*, 4692–4700.
[14] E. J. Jo, N. Fuller, R. P. Rand, P. St George-Hyslop, P. E. Fraser, *J. Mol. Biol.* **2002**, *315*, 799–807.
[15] V. Narayanan, S. Scarlata, *Biochemistry* **2001**, *40*, 9927–9934.
[16] M. Ramakrishnan, P. H. Jensen, D. Marsh, *Biochemistry* **2006**, *45*, 3386–3395.
[17] M. Ramakrishnan, P. H. Jensen, D. Marsh, *Biochemistry* **2003**, *42*, 12919–12926.
[18] R. Bussell, T. F. Ramlall, D. Eliezer, *Protein Sci.* **2005**, *14*, 862–872.
[19] P. Borbat, T. F. Ramlall, J. H. Freed, D. Eliezer, *J. Am. Chem. Soc.* **2006**, *128*, 10004–10005.
[20] S. Chandra, X. C. Chen, J. Rizo, R. Jahn, T. C. Südhof, *J. Biol. Chem.* **2003**, *278*,15313–15318.
[21] T. S. Ulmer, A. Bax, *J. Biol. Chem.* **2005**, *280*, 43179–43187.
[22] J. Bhatnagar, J. H. Freed, B. R. Crane, *Methods Enzymol.* **2007**, *423*, 117–133.
[23] C. C. Jao, A. Der-Sarkissian, J. Chen, R. Langen, *Proc. Natl. Acad. Sci. USA* **2004**, *101*, 8331–8336.
[24] A. Der-Sarkissian, C. C. Jao, J. Chen, R. Langen, *J. Biol. Chem.* **2003**, *278*, 37530–37535.
[25] M. Margittai, R. Langen, *Methods Enzymol.* **2006**, *413*, 122–139.
[26] M. Margittai, R. Langen, *J. Biol. Chem.* **2006**, *281*, 37820–37827.
[27] C. Altenbach, T. Marti, H. G. Khorana, W. L. Hubbell, *Science* **1990**, *248*, 1088–1092.
[28] R. J. Perrin, W. S. Woods, D. F. Clayton, J. M. George, *J. Biol. Chem.* **2000**, *275*, 34393–34398.
[29] C. S. Klug, J. B. Feix, *Protein Sci.* **1998**, *7*, 1469–1476.
[30] K. B. Qu, J. L. Vaughn, A. Sienkiewicz, C. P. Scholes, J. S. Fetrow, *Biochemistry* **1997**, *36*, 2884–2897.
[31] R. Langen, K. W. Cai, C. Altenbach, H. G. Khorana, W. L. Hubbell, *Biochemistry* **1999**, *38*, 7918–7924.
[32] H. S. Mchaourab, M. A. Lietzow, K. Hideg, W. L. Hubbell, *Biochemistry* **1996**, *35*, 7692–7704.
[33] S. Kubo, V. M. Nemani, R. J. Chalkley, M. D. Anthony, N. Hattori, Y. Mizuno, R. H. Edwards, D. L. Fortin, *J. Biol. Chem.* **2005**, *280*, 31664–31672.
[34] M. Bisaglia, E. Schievano, A. Caporale, E. Peggion, S. Mammi, *Biopolymers* **2006**, *84*, 310–316.
[35] S. Stoll, A. Schweiger, *J. Magn. Reson.* **2006**, *178*, 42–55.
[36] S. Steigmiller, M. Börsch, P. Gräber, M. Huber, *Biochim. Biophys. Acta Bioenerg.* **2005**, *1708*, 143–153.

Received: April 10, 2008
Published online on September 26, 2008

